Rodrigue Matadi Boumbimba
IMFS,
University of Strasbourg,
2 Rue Boussingault,
67000 Strasbourg, France

Said Ahzi
IMFS,
University of Strasbourg,
2 Rue Boussingault,
67000 Strasbourg, France;
TEMA,
Department of Mechanical Engineering,
University of Aveiro,
3810-193 Aveiro, Portugal

Nadia Bahlouli[1]
IMFS,
University of Strasbourg,
2 Rue Boussingault,
67000 Strasbourg, France
e-mail: nadia.bahlouli@unistra.fr

David Ruch
LTI,
Public Research Center Henry Tudor,
70 Rue de Luxembourg,
L-4221 Esch-sur-Alzette, Luxembourg

José Gracio
TEMA,
Department of Mechanical Engineering,
University of Aveiro,
3810-193 Aveiro, Portugal

Dynamic Mechanical Properties of PMMA/Organoclay Nanocomposite: Experiments and Modeling

Similarly to unfilled polymers, the dynamic mechanical properties of polymer/organoclay nanocomposites are sensitive to frequency and temperature, as well as to clay concentration. Richeton et al. (2005, "A Unified Model for Stiffness Modulus of Amorphous Polymers Across Transition Temperatures and Strain Rates," Polymer, 46, pp. 8194–8201) has recently proposed a statistical model to describe the storage modulus variation of glassy polymers over a wide range of temperature and frequency. In the present work, we propose to extend this approach for the prediction of the stiffness of polymer composites by using two-phase composite homogenization methods. The phenomenological law developed by Takayanagi et al., 1966, J. Polym. Sci., 15, pp. 263–281 and the classical bounds proposed by Voigt, 1928, Wied. Ann., 33, pp. 573–587 and Reuss and Angew, 1929, Math. Mech., 29, pp. 9–49 models are used to compute the effective instantaneous moduli, which is then implemented in the Richeton model (Richeton et al., 2005, "A Unified Model for Stiffness Modulus of Amorphous Polymers Across Transition Temperatures and Strain Rates," Polymer, 46, pp. 8194–8201). This adapted formulation has been successfully validated for PMMA/cloisites 20A and 30B nanocomposites. Indeed, good agreement has been obtained between the dynamic mechanical analysis data and the model predictions of poly(methyl-methacrylate)/organoclay nanocomposites.
[DOI: 10.1115/1.4004052]

Keywords: PMMA, organoclay, polymer nanocomposites, storage modulus, micromechanical modeling

1 Introduction

Montmorillonite organoclay is one of the most useful fillers for the preparation of polymer/clay nanocomposites. This filler exhibits a large stiffness and large specific area that can lead to the enhancement of the mechanical properties [1]. Many experimental works reported in the literature have shown an enhancement of the stiffness and hardness compared to the polymer matrix [2–7]. For example, in our previous work [8], we have shown that the storage modulus of both PMMA/C20A and PMMA/C30B increases with the organoclay concentration. This enhancement in properties has led Toyota research group to develop an industrial process for manufacture of polymer/clay nanocomposites [7,9]. However, synthesis and characterization of polymer based nanocomposites demand the use of sophisticated processing methods and testing equipments, which could result in valuable costs. For this reason, the development of constitutive model for the determination of mechanical properties, such as storage modulus, has proven to be very effective [10–17]. The introduction of these constitutive laws in computational modeling can facilitate the design and development of nanocomposite structures for engineering applications.

Many models have been developed to predict the stiffness of polymers. A review of these models was reported by Keller et al. [18,19]. Drozdov [20] proposed the following temperature dependence for the Young's modulus:

$$E(T) = E_0 - \frac{E_1}{T_g - T} \tag{1}$$

where E_0 and E_1 are material parameters and T_g is the glass transition temperature. However, this equation can only be used to describe the very beginning of the glass transition but not the rubbery plateau.

Among the existing models, only Mahieux and Reifsnider [21,22] works are valid from glassy to rubbery state of the polymers. These authors have developed a statistical model for temperature dependence of the storage modulus. Their idea was to use Weibull statistical to represent the failure of secondary bonds during the relaxation processes that leads to the stiffness change. Starting from the Mahieux and Reifsnider [21] equation, Richeton et al. [23] suggest the following temperature and frequency dependence for the storage modulus E:

$$\begin{aligned} E(T, f) = {} & (E_1(f) - E_2(f)) \cdot \exp\left(-\left(\frac{T}{T_\beta(f)}\right)^{m_1}\right) \\ & + (E_2(f) - E_3(f)) \cdot \exp\left(-\left(\frac{T}{T_g(f)}\right)^{m_2}\right) \\ & + E_3(f) \cdot \exp\left(-\left(\frac{T}{T_f(f)}\right)^{m_3}\right) \end{aligned} \tag{2}$$

where T_β is the β transition temperature, T_g is the glass transition temperature, and T_f is the temperature marking the beginning of the flow region. The moduli E_i are the instantaneous storage moduli of the material at the beginning of each region. The parameters m_i are the Weibull moduli, corresponding to the statistics of the bond breakage. The expressions of T_β, T_g, and T_f are given in Eqs. (3)–(5), respectively

[1]Corresponding author.

Contributed by the Materials Division of ASME for publication in the JOURNAL OF ENGINEERING MATERIALS AND TECHNOLOGY. Manuscript received May 18, 2010; final manuscript received March 3, 2011; published online July 18, 2011. Assoc. Editor: Hussein Zbib.

$$\frac{1}{T_\beta} = \frac{1}{T_\beta^{\text{ref}}} + \frac{k}{\Delta H_\beta} \ln\left(f^{\text{ref}}/f\right) \tag{3}$$

$$T_g = T_g^{\text{ref}} + \frac{-c_2^{\text{ref}} \cdot \log\left(f^{\text{ref}}/f\right)}{c_1^{\text{ref}} + \log\left(f^{\text{ref}}/f\right)} \tag{4}$$

$$T_f = T_f^{\text{ref}} \cdot \left(1 + 0.01 \cdot \log\left(f/f^{\text{ref}}\right)\right) \tag{5}$$

The parameter f^{ref} represents the reference frequency. The parameters c_1^{ref} and c_2^{ref} are the Williams–Landel–Ferry (WLF) parameters relative to T_g. The parameters T_β^{ref} and T_g^{ref} are β transition and glass transition temperatures at the reference frequency f^{ref}. ΔH_β is the β activation energy. In our study, we took the effective activation energy to calculate secondary transition temperature $T_\beta(f)$ of the nanocomposites. The values of β effective activation energy are given in a previous work [24]. The moduli, E_i, are the instantaneous storage moduli of the material at the beginning of each region and are given by

$$E_i = E_i^{\text{ref}} \cdot \left(1 + s \cdot \log\left(f/f^{\text{ref}}\right)\right) \tag{6}$$

where E_i^{ref} represent the instantaneous storage moduli at the reference frequency and s is the sensitivity of the storage modulus to frequency. Richeton et al. [23] assumed that s is a constant parameter for a given polymer.

This model has given good results for the prediction of the storage modulus of three amorphous polymers poly(methyl methacrylate) (PMMA, Polycarbonate (PC), and Polyamide-imide (PAI)). In this work, we suggest to extend this model for the prediction of the storage modulus of polymer organoclay nanocomposites, by using homogenization methods. Both Takayanagi et al. [25] and the classical bounds theories of Voigt [26] (upper bound) and Reuss et al. [27] (lower bound) are used to compute the effective's instantaneous modulus, which is then implemented in the Richeton model [23].

2 Dynamic Mechanical Analysis

2.1 Experiments. The two nanocomposites studied in this work, are obtained by the melt intercalation of PMMA and two organoclay supplied by Southern clay products, USA): Cloisite 20A (C20A) (Montmorillonite (MMT)-Alk; modified by dimethyl 2-ethyl-hexyl (hydrogenated tallowalkyl) ammonium cation) and cloisite 30B (C30B) (MMT–$(OH)_2$; modified by methyl bis (2-hydroxyethyl) (hydrogenated tallowalkyl) ammonium cation. The content of modified montmorillonite clays varies from 1 wt. % to 5 wt. %. The dispersion and the layer conformation of the cloisites in the nanocomposites were characterized by X-ray diffraction and transmission electron microscopy (TEM). Both X-ray and TEM depicted an exfoliated morphology in case of PMMA/C30B nanocomposites and an intercalated structure in the case of PMMA/C20A organoclay nanocomposites (see Fig. 1). Detailed informations about the material preparation and the morphology characterization have been reported in our first paper [8].

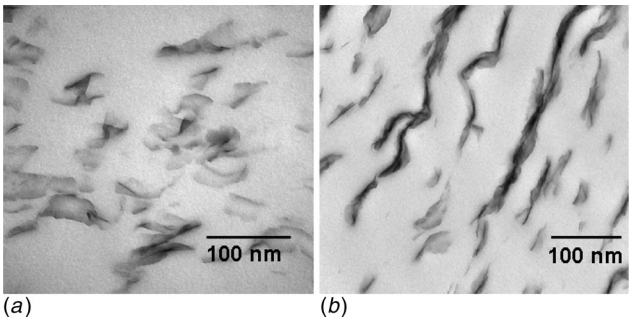

(*a*) (*b*)

Fig. 1 TEM images of PMMA organoclay nanocomposites at high magnification: (*a*) PMMA/C30B and (*b*) PMMA/C20A, showing the exfoliated and intercalated morphology, respectively

Dynamic mechanical analysis was performed on a Netzch DMA 242C dynamic mechanical analyzer (DMA). The dynamic temperature spectra of the nanocomposites are obtained in three-point bending mode at different vibration frequencies, with a constant static force of 0.5 N, for a temperature range of $-50\,^\circ\text{C} \sim 150\,^\circ\text{C}$, and a heating rate of $1\,^\circ\text{C}$/min in a nitrogen atmosphere. The specimens used for the DMA are obtained by melt injection molding with dimensions of 60 mm × 10 mm × 3 mm. The effect of clay concentration on both storage modulus and glass transition temperature has been studied in Matadi et al. [8]. In this work, we focus our attention on the frequency effect on both storage modulus and glass transition temperature of the two nanocomposites obtained.

2.2 Modeling of Temperature and Frequency Effect on the Storage Modulus. Like unfilled polymers, the viscoelastic properties of polymer/clay nanocomposites are very sensitive to frequency and temperature. This led us to use the form of Richeton model [23] for the prediction of their storage modulus. The effect of clay concentration on the storage modulus has been introduced in the Eq. (2) by replacing the instantaneous storage modulus present in Eq. (2) by their effective values. The resulted formulation is given by

$$\begin{aligned} E(T,f) = {} & \left(E_{1\text{eff}}(f) - E_{2\text{eff}}(f)\right) \cdot \exp\left(-\left(\frac{T}{T_\beta(f)}\right)^{m_1}\right) \\ & + \left(E_{2eff}(f) - E_{3\text{eff}}(f)\right) \cdot \exp\left(-\left(\frac{T}{T_g(f)}\right)^{m_2}\right) \\ & + E_{3\text{eff}}(f) \cdot \exp\left(-\left(\frac{T}{T_f(f)}\right)^{m_3}\right) \end{aligned} \tag{7}$$

In Eq. (6), E_i and E_i^{ref} are linked. Thus, calculating the effective values of E_i corresponds to calculate the effective values of E_i^{ref}.

2.3 Modeling of the Effective Parameters. The extension of the "Richeton" model [23] to predict the storage modulus of the nanocomposites may be possible by the way of the calculation of the effective instantaneous modulus. The issue is how to choose the best model for the prediction of effective modulus that can lead to a good determination of the storage modulus of PMMA/C30B and PMMA/C20A organoclay nanocomposites. We consider the polymer nanocomposites as a two phase material where the storage modulus is described by the contribution of the two phases. As a first homogenization method, we propose to use the

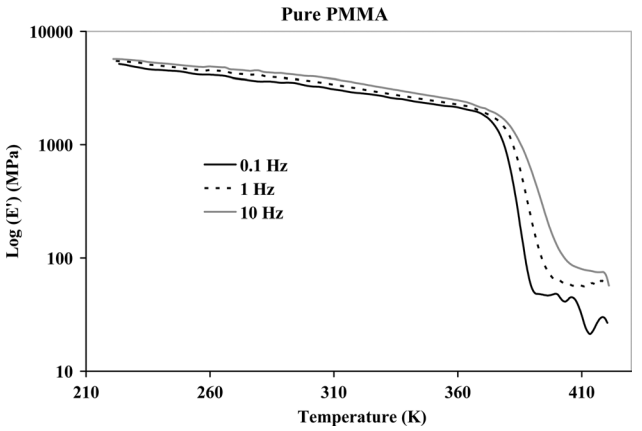

Fig. 2 Experimental results for the storage modulus of PMMA at different frequencies

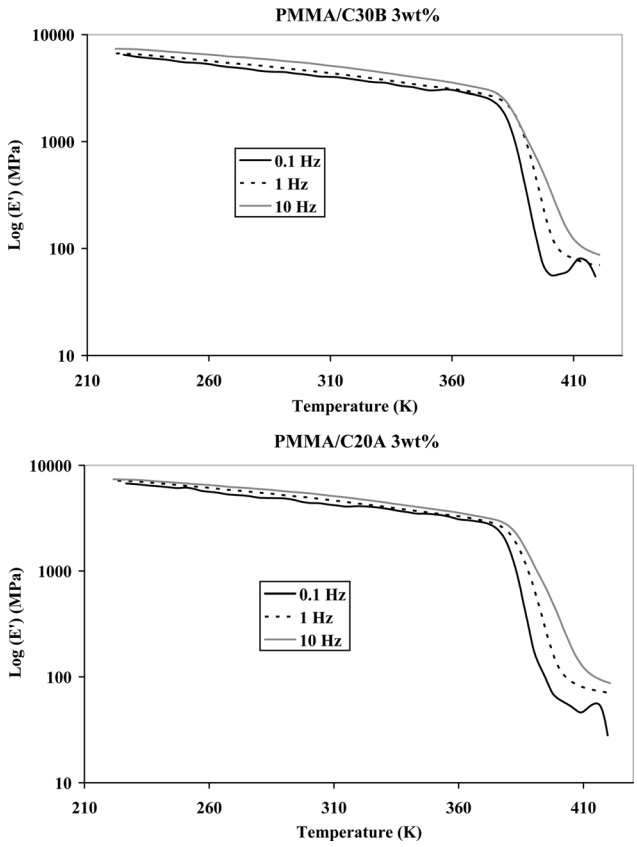

Fig. 3 Experimental results for the storage modulus of PMMA/C20A and PMMA/C30B organoclay nanocomposites at different frequencies

classical bounds theories of Voigt [26] (upper bound) and Reuss [27] (lower bound).

$$\begin{cases} E_{1\text{eff}}^{\text{UB}} = f_m . E_{1m} + f_c . E_{1c} \\ E_{2\text{eff}}^{\text{UB}} = f_m . E_{2m} + f_c . E_{2c} \\ E_{3\text{eff}}^{\text{UB}} = f_m . E_{3m} + f_c . E_{3c} \end{cases} \tag{8}$$

$$\begin{cases} E_{1\text{eff}}^{\text{LB}} = (f_m / E_{1m} + f_c / E_{1c})^{-1} \\ E_{2\text{eff}}^{\text{LB}} = (f_m / E_{2m} + f_c / E_{2c})^{-1} \\ E_{3\text{eff}}^{\text{LB}} = (f_m / E_{3m} + f_c / E_{3c})^{-1} \end{cases} \tag{9}$$

In those equations, f_m and f_c are the volume fraction of the PMMA matrix and the volume fraction of the organoclay phases, respectively, with $f_m + f_c = 1$. The subscripts "UB" and "LB" refer to upper bound and lower bound, m to matrix, and c to clay. The E_{im} and E_{ic} with i from 1 to 3 represent the instantaneous storage moduli of the PMMA and the organoclay, respectively. We assume

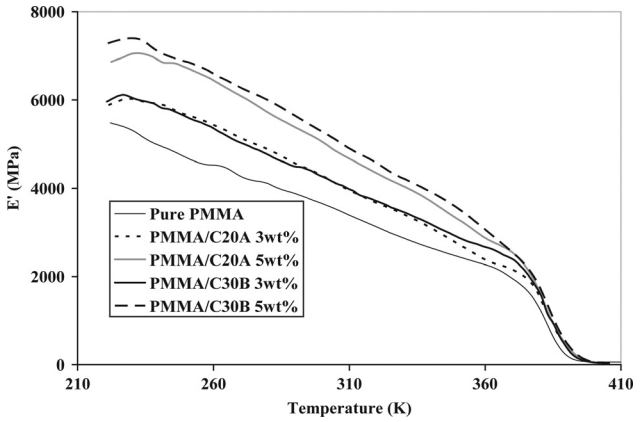

Fig. 4 Storage modulus versus temperature of both PMMA/C20A and PMMA/C30B at different organoclay concentrations and at a frequency of 1 Hz

that the modulus of the organoclay are not sensitive to the frequency and the temperature. This allows us to take. $E_{1c} = E_{2c} = E_{3c} = E_{\text{clay}}$.

The second homogenization model is the phenomenological law developed by Takayanagi et al. [25]. This model comes from the mixture of Voigt and Reuss theories. It is usually expressed to represent the shear modulus of composite materials. In this work, we adapted it for the description of $E_{1\text{eff}}$, $E_{2\text{eff}}$, and $E_{3\text{eff}}$ as follows:

$$\begin{cases} E_{1\text{eff}} = \dfrac{\varphi . E_{1c} . E_{1m}}{\Omega . E_{1m} + (1-\Omega) . E_{1c}} + (1-\varphi) . E_{1m} \\ E_{2\text{eff}} = \dfrac{\varphi . E_{2c} . E_{2m}}{\Omega . E_{2m} + (1-\Omega) . E_{2c}} + (1-\varphi) . E_{2m} \\ E_{3\text{eff}} = \dfrac{\varphi . E_{3c} . E_{3m}}{\Omega . E_{3m} + (1-\Omega) . E_{3c}} + (1-\varphi) . E_{3m} \end{cases} \tag{10}$$

In this expression, φ and Ω are parameters related to the organoclay and PMMA matrix volume fractions

$$\begin{cases} f_c = \varphi \, . \, \Omega \\ f_m = 1 - \varphi \, . \, \Omega \end{cases} \tag{11}$$

After calculating the effective parameters, the storage modulus is then derivated by inserting the expression given by Eqs. (8)–(10) in the Richeton model [23] as described by Eq. (7). In what follows, these models are referred as Richeton modified Voigt model (RVM), Richeton modified Reuss model (RRM), and Richeton modified Takayanagi model (RTM). To compute the volume fraction of the organoclay as function of the clay content in weight percentage, the following relation is used (Eq. (12) [28]):

$$f_c = w_c [w_c + (1 - w_c)\, \rho_c / \rho_m]^{-1} \tag{12}$$

Table 1 Takayanagi–Richeton modified model parameter for the nanocomposites at 1 Hz

	PMMA/C30B 3 wt. %	PMMA/C30B 5 wt. %	PMMA/C20A 3 wt. %	PMMA/C20A 5 wt. %
E_{clay}(MPa)	8×10^4	8×10^4	8×10^4	8×10^4
f_c	1.28×10^{-2}	2.17×10^{-2}	1.28×10^{-2}	2.17×10^{-2}
Ω	0.036	0.061	0.036	0.061
φ	0.827	0.827	0.827	0.827
$E_{1\text{eff}}^{\text{ref}}$(MPa)	7114	7293.84	7114.38	7293.84
$E_{2\text{eff}}^{\text{ref}}$(MPa)	3428	3454.30	3428.15	3454.30
$E_{3\text{eff}}^{\text{ref}}$(MPa)	141	142	141	142
$\Delta H_{\beta\text{eff}}$ (kJ/mol)	103	106	103	106
T_g^{ref}	397	398	395	397

Table 2 Parameters for the modeling of the storage modulus of pure PMMA at 1 Hz

	PMMA
f^{ref} (Hz)	1
E_1^{ref} (MPa)	5478
E_2^{ref} (MPa)	2623
E_3^{ref} (MPa)	107
T_β^{ref} (K)	305
T_g^{ref} (K)	391
T_f^{ref} (K)	410
m_1	7
m_2	41
m_3	8
s	0.087
ΔH_β(kJ/mol)	100
c_1^g	60
c_2^g(°C)	2.9
ρ_m(g/cm^3)	1.19
ρ_f(g/cm^3)	2.83

where f_c is the volume fraction of particles and W_c is the weight fraction of particles. ρ_c and ρ_m represent the density of particles and PMMA matrix, respectively.

3 Results and Discussion

3.1 Temperature and Frequency Effects. Figures 2 and 3 represent the storage modulus obtained for pure PMMA and for the nanocomposites PMMA/C20A and PMMA/C30B determined by DMA. Like the pure PMMA the PMMA/organoclay nanocomposites are sensitive to the temperature and frequency. Both storage modulus and the glass transition temperature increase with increasing frequency. The figures also depict the decrease of the storage modulus with increasing temperature. Figure 4 shows the storage modulus of both PMMA/C20A and PMMA/C30B organoclay nanocomposites for different organoclay concentrations. It clearly appears that the storage modulus increases with increasing organoclay concentration for both nanocomposites. However, we can note that there is a slight increase between 3 wt. % and 5 wt. % of organoclay concentrations, probably due to the presence of aggregates at 5 wt. % of filler concentration. In a previous work [8], we have shown that the glass transition temperature of the two organoclay nanocomposites obtained shifts to higher values. The values of T_g increase from 118.6 °C for the pure PMMA, to 123.8 °C and 122.4 °C, respectively, for PMMA/C30B and PMMA/C20A with only 1 wt. % of organoclays content. Beyond 1 wt. % of organoclays content, the T_g varies very slightly with the clays content. Information depicted by the experimental results (Figs. 2 and 3) is that the PMMA and the two nanocomposites obtained appear to have approximately the same frequency sensitivity. One can see this effect on the glassy region for example. From the experimental results depicted in Fig. 4, the storage modulus of PMMA/C30 with 3 wt. % (exfoliated) seems to be slightly different to that of PMMA/C20A with 3 wt. % (intercalated). The same tendency is observed for 5 wt. % of organoclay concentration. This observation leads us to suggest that the nanocomposites morphology seems to slightly affect the storage modulus (Figs. 2–4).

3.2 Identification of the Model Parameters. Like in the works of Mahieux and Reifsnider [21,22] and Richeton et al. [23], for the model parameters determination, we chose to divide

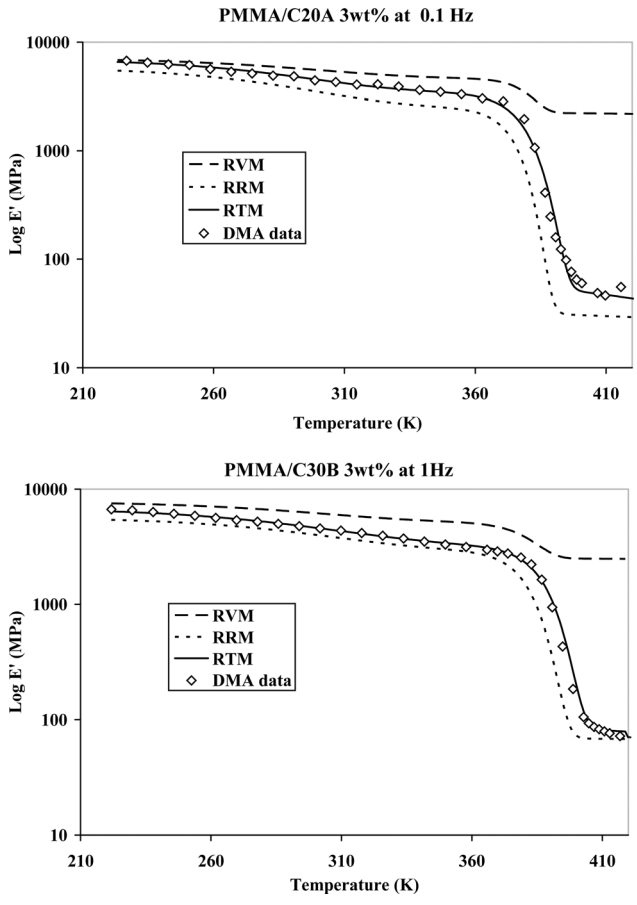

Fig. 5 Models predictions of the storage modulus as function of temperature for PMMA/C20A and PMMA/C30B nanocomposites

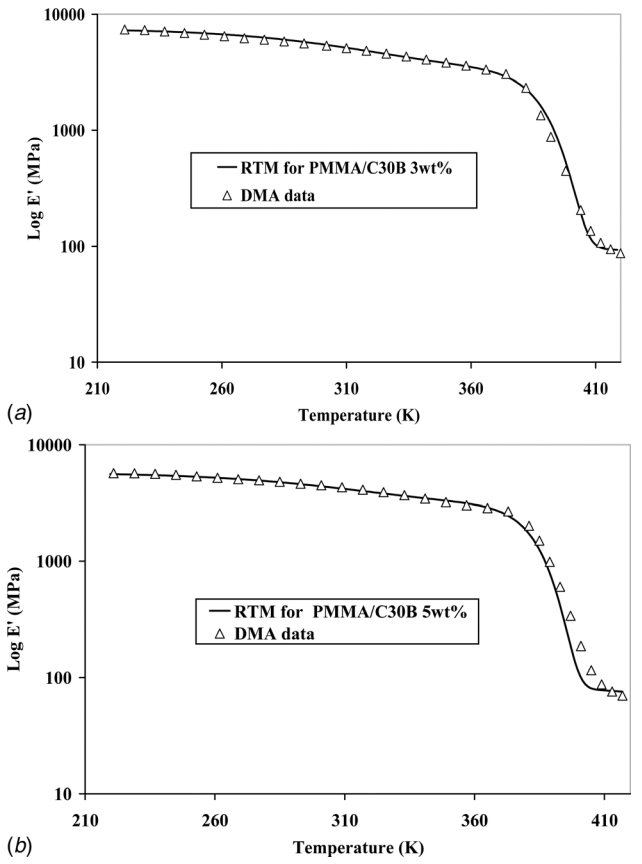

Fig. 6 Model prediction of the he storage modulus as function of temperature for the PMMA/C30B nanocomposites at a frequency of 1 Hz, (*a*) at 3 wt. % of organoclay concentration and (*b*) at 5 wt. % of organoclay concentration

them into two types: physical parameters and statistical parameters. All of the physical parameters can be determined by DMA experimental results. Both instantaneous modulus and glass transition temperature values of the PMMA matrix have been taken from the DMA results. Like in Richeton et al. [23], we also chose to take an intermediate value for the reference frequency. A value of 1 Hz for f^{ref} appears a good choice. After the determination of the instantaneous modulus values of PMMA matrix, the correspondent values of the two nanocomposites have been obtained by using the Takayanagi or classical bounds homogenization models. For the Takayanagi model, the fitting parameter φ for 3 wt. % and 5 wt. % organoclay content is reported in Table 1. The frequency sensitivity was obtained from an average value of experimental data. For the value of the effective activation energy $\Delta H_{\beta\mathrm{eff}}$, we took the values from our previous study on the yield stress Matadi et al. [24]. The values of c_2^{ref} and c_1^{ref} have been determined from experimental results on glass transition temperature T_g of both pure PMMA and the organoclay nanocomposites.

We took the Weibull moduli m_i, corresponding to the statistics of the bond breakage from the work of Richeton et al. [23] on the PMMA. However, our values (Table 2) are slightly higher. All model parameters are given in Table 2.

3.3 Discussion. Figure 5 represents the storage modulus as a function of temperature built with the three different micromechanical approaches for PMMA/C20A and PMMA/C30B at a frequency of 0.1 Hz and 1 Hz, respectively. As expected, the RTM lies between the upper RVM and the lower RRM bound models. One can clearly observe that the RTM provides a good fitting of experimental data. For the clarity reasons, in the rest of this work we will only display the results of Takayanagi modified Richeton model. Figures 6 and 7 represent the computed data of the storage modulus of PMMA/C20A and PMMA/C30B at a frequency of 1 Hz and at different organoclay concentration. The model predictions are in good agreement with DMA data. Figures 8 and 9 show the comparisons of the storage modulus at various frequencies, from 0.1 Hz to 10 Hz as described by the model, Eq. (7), and the corresponding experimental results for PMMA/C30B 3 wt. %, PMMA/C30B 5 wt. %, PMMA/C20A 3 wt. %, PMMA/C20A 5 wt. %, respectively. It is observed that the Takayanagi-modified Richeton model accurately describes the storage modulus of the two organoclay nanocomposites. This good fitting of experimental data by the model confirms our assumption that there is no strong interaction between the organoclay layers and the PMMA matrix. Moreover, the addition of organoclay does not affect the activation process conducting to the different transition. In fact, the increase of mechanical and thermal properties is strongly related to the good dispersion of nanosize organoclay particles, which restricts the polymer chain mobility under loading [29]. Going from this assumption, it is very simple to understand why the clay addition does not have a significant effect on the Weibull modulus. In the works of Mahieux and Reifsnider [21,22], Mahieux [30] and Burdette [31] on the modeling of the storage modulus of conventional composites, the molecular weight, the rate of crystallinity, and filler concentration are found to have a great effect on the Weibull moduli. However, in our case, the addition of organoclay in the PMMA matrix leads to slight change in molecular weight, and the enhancement in properties seems not to depend on the type of nanocomposites morphology (intercalated or exfoliated) (Fig. 1). This RTM possesses a relatively simple form with reasonable number of parameters, which makes it feasible to the introduction in a numerical simulation codes for the purposes of engineering design and optimization.

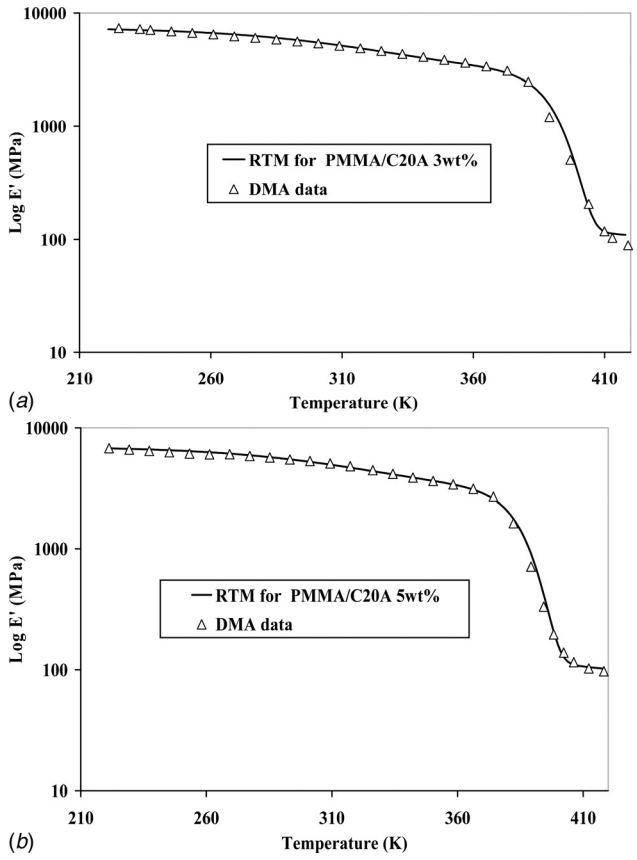

Fig. 7 Model prediction of the storage modulus as function of temperature for the PMMA/C20A nanocomposite at a frequency of 1 Hz: (*a*) at 3 wt. % of organoclay concentration and (*b*) at 5 wt. % of organoclay concentration

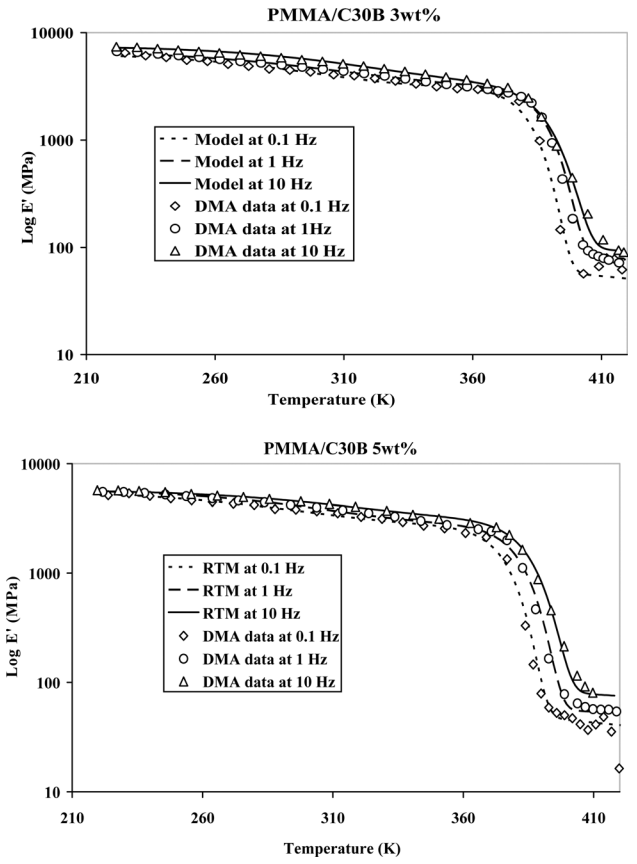

Fig. 8 Model prediction and experimental data of the storage modulus as function of temperature for PMMA/C30B nanocomposites at different frequencies

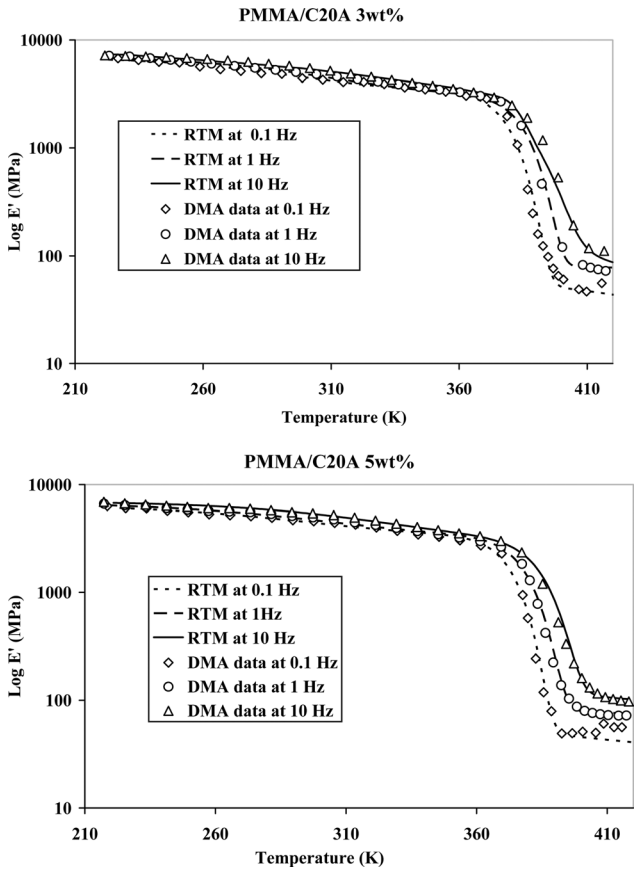

Fig. 9 Model prediction and experimental data of the storage modulus as function of temperature for PMMA/C20A nanocomposites at different frequencies

4 Conclusion

Frequency and temperature dependent storage modulus of PMMA, PMMA/C30B, and PMMA/C20A organoclay nanocomposites was investigated over a broad range of frequency and temperature using the dynamical mechanical analysis.The results obtained by DMA tests show that the storage modulus of the two organoclay nanocomposites is very sensitive to frequency, temperature and clay concentration. Using Takayanagi and classical bounds homogenization methods to take into account of organoclay concentration effect, the Richeton model for the prediction of amorphous polymers storage modulus has been extended to polymer organoclay nanocomposites. As expected, the RTM lies between the upper and the lower bound models (RVM and RRM). The RTM provides a very good accuracy with the experimental data, for the two nanocomposites, for different frequencies and for different clay concentrations. This model is a first step to understand the behavior of polymers organoclay nanocomposites. The results presented in this work lead us to believe that the enhancement in properties for PMMA/cloisites organoclay nanocomposites are more related to the good dispersion of organoclay fillers than to the presence interaction links between the organoclay and the PMMA matrix.

References

[1] Chen, B., and Evans, J. R. G., 2006, "Elastic Moduli of Clay Platelets," Scr. Mater., **54**(9), pp. 1581–1585.

[2] Ginzburg, V. V., Singh, C., and Balazs, A. C., 2000, "Theoritical Phase Diagrams of Polymer/Clay Composites: The Role of Grafted Orgaanic Modifiers," Macromolecules, **33**, pp. 1089–1099.

[3] Giannelis, E. P., 1996, "Polymer Layered Silicate Nanocomposites," Adv. Mater., **8**, pp. 29–35.

[4] Chen, G., and Qi, Z., 2000, "Shear-Induced Ordered Structure in Polystyrene/Clay Nanocomposite," J. Mater. Res., **15**, pp. 351–356.

[5] Ma, J., Qi, Z., and Hu, Y, 2001, "Synthesis and Characterization of Polypropylene/Clay Nanocomposites," J. Appl. Polym. Sci., **82**, pp. 3611–3617.

[6] Lan, T., and Pinnavaia, T. J., 1994, "Clay-Reinforced Epoxy Nanocomposites," Chem. Mater., **6**, pp. 2216–2219.

[7] Kojima, Y., Kawasumi, M., Usuki, A., Okada, A., Fukushima, Y. Kurachi, T., and Kamigaito, O., 1993, "Mechanical Properties of Nylon 6-Clay Hybrid," J. Mater. Res., **8**, pp. 1185–1189.

[8] Matadi, R., Makradi, A., Ahzi, S., Sieffert, J. G., Etienne, S., Rush D., Vaudemont, R., Muller, R., and Bouquey, M., 2009, "Preparation, Structural Characterization, and Thermomechanical Properties of Poly(Methyl Methacrylate)/Organoclay Nanocomposites by Melt Intercalation," J. Nanosci. Nanotechnol., **9**, pp. 2923–2930.

[9] Usuki, A., Kojima, Y., Kawasumi, M., Okada, A., Fukushima, Y., Kurauchi, T., and Kamigaito, O., 1993, "Synthesis of Nylon 6-Clay Hybrid," J. Mater. Res., **8**, pp. 1179–1184.

[10] Liu, Y. J., and Chen, X. L., 2003, "Evaluations of the Effective Material Properties of Carbon Nanotube-Based Composites Using a Nanoscale Representative Volume Element," Mech. Mater., **35**, pp. 69–81.

[11] Chen, X. L., and Liu, Y. J., 2004, "Square Representative Volume Elements for Evaluating the Effective Material Properties of Carbon Nanotube-Based Composites," Comput. Mater. Sci., **29**, pp. 1–11.

[12] Liu, Y., Nishimura, N., and Otani, Y., 2005, "Large-Scale Modeling of Carbon-Nanotube Composites by the Boundary Element Method Based on a Rigid-Inclusion Model," Comput. Mater. Sci., **34**, pp. 173–187.

[13] Van Workum, K., and de Pablo, J. J., 2003, "Computer Simulation of the Mechanical Properties of Amorphous Polymer Nanostructures," Nano Lett., **3**, pp. 1405–1410.

[14] Ospina, S. A., Restrepo, J., and Lopez, B. L., 2003, "Deformation of Polyethylene: Monte Carlo Simulation," Mater. Res. Innovations, **7**, pp. 27–30.

[15] Sheng, N., Boyce, M. C., and Parks, D. M., 2004, "Multiscale Micromechanical Modeling of Polymer/Clay Nanocomposites and the Effective Clay Particle," Polymer, **45**, pp. 487–506.

[16] Gates, T. M., and Hinkley, J. A., 2003, "Computational Materials: Modeling and Simulation of Nanostructured Materials and Systems," NASA/TM–212163.

[17] Odegard, G. M., Gates, T. S., Wise, K. E., Park, C., and Siochi, E. J., 2003, "Constitutive Modeling of Nanotube-Reinforced Polymer Composites," Compos. Sci. Technol., **63**, pp. 1671–1687.

[18] Keller, T., Tracy, C., and Zhou, A., 2006, "Structural Response of Liquid-Cooled GFRP Slabs Subjected to Fire—Part I: Material and Post-Fire Modeling," Composites Part A, **37**(9), pp. 1286–95.

[19] Keller, T., Tracy, C., and Zhou, A., 2006, "Structural Response of Liquid-Cooled GFRP Slabs Subjected to Fire - Part II: Thermo-Chemical and Thermo-Mechanical Modeling," Composites Part A, **37**(9), pp. 1296–308.

[20] Drozdov, A. D., 2000, "Viscoelastoplasticity of Amorphous Glassy Polymers," Eur. Polym. J., **36**, pp. 2063–2074.

[21] Mahieux, C. A., and Reifsnider, K. L., 2001, "Property Modeling Across Transition Temperatures in Polymers: A Robust Stiffness—Temperature Model," Polymer, **42**, pp. 3281–3291.

[22] Mahieux, C. A., and Reifsnider, K. L., 2002, "Property Modeling Across Transition Temperatures in Polymers: Application to Thermoplastic Systems," J. Mater. Sci., **37**, pp. 911–920.

[23] Richeton, J., Schlatter, G., Vecchio, K. S., Rémond, Y., and Ahzi, S., 2005, "A Unified Model for Stiffness Modulus of Amorphous Polymers Across Transition Temperatures and Strain Rates," Polymer, **46**, pp. 8194–8201.

[24] Matadi, R., Gueguen, O., Ahzi, S., Gracio, J., and Ruch, D., 2010, "Investigation of the Stiffness and Yield Behaviour of Melt-Intercalated Poly (Methyl Methacrylate)/Organoclay Nanocomposites: Characterisation and Modelling," J. Nanosci. Nanotechnol, **10**, pp. 2956–2961.

[25] Takayanagi, M., Harima, H., and Iwata, Y., 1963, "Viscoelastic Behaviour of Polymer Blends and Its Comparison With Model Experiments," *Memoirs of the Faculty of Engineering, Kyushu University*, **23**, pp. 1–13.

[26] Voigt, W., 1889, "Über die Beziehung zwischen den beiden Elastizitätskonstanten isotroper Körper," Wied. Ann., **38**, pp. 573–587.

[27] Reuss, A., 1929, "Berechnung der Fließgrenze von Mischkristallen auf Grund der Plastizitätsbedingung für Einkristalle," Z. Angew. Math. Mech., **9**, pp. 49–58.

[28] Goyal, R. K., Tiwari, A. N., and Negi, Y. S., 2008, "Microhardness of PEEK/Ceramic Micro- and Nanocomposites: Correlation With Halpin–Tsai Model," Mater. Sci. Eng., **491**, pp. 230–236.

[29] Wei, C. L., Zhang, M. Q., Rong, M. Z., and Friedrich, K., 2002, "Tensile Performance Improvement of Low Nanoparticles Filled-Polypropylene Composites," Compos. Sci. Technol., **62**, pp. 1327–1340.

[30] Mahieux, C. A., 1999, "A Systematic Stiffness-Temperature Model for Polymers and Applications to the Prediction of Composite Behavior," Ph.D. dissertation, Virginia Polytechnic Institute and State University; 1999. Blacksburg, VA 24061-0002.

[31] Burdette, J. A., 2001, "Fire Response of Loaded Composite Structures—Experiments and Modeling," Master thesis, Virginia Polytechnic Institute and State University; 2001. Blacksburg, VA 24061-0002.